Journal of Climate Change and Space Science *(JCCaSS)* 2(1)(2026): 3
https://doi.org/10.17576/jccass.0201.2026.03

Patterns and Trends in Total Electron Content over Malaysia Region: A 12 Year Analysis

Siti Aminah Bahari[a*], Mardina Abdullah[a,b] , & Tajul Ariffin Musa[c]

[a]*Space Science Centre, Institute of Climate Change, The University of Malaysia, Bangi, Selangor, Malaysia*
[b]*Department of Electrical, Electronic and Systems Engineering, Faculty of Engineering and Built Environment, The University of Malaysia, Bangi, Selangor, Malaysia*
[c]*Centre of Tropical Geoengineering (GEOTROPIK), Faculty of Built Environment and Surveying, Universiti Teknologi Malaysia, Skudai, Johor, Malaysia*
**Corresponding author: sitiaminahbahari@ukm.edu.my*

Received: 6 November 2024; Accepted: 21 January 2026; Published: 31 January 2026

ABSTRACT

The ionosphere, one of the Earth's atmosphere, plays a vital role in the equatorial atmosphere and influenced by solar radiation. One key parameter used to describe this ionized layer is the Total Electron Content (TEC), which directly affects the transmission of electromagnetic signals such as satellite navigation systems. A comprehensive understanding of the TEC behavior is essential to improve in modeling the ionosphere and reduce errors in satellite-based communications. Despite its importance, long-term analyses of TEC variations over equatorial region, especially Malaysia, which is situated close to the geomagnetic equator, remain limited. This study addresses this gap by examining over a decade of TEC observations from 2003 to 2014. TEC were computed using Bernese GPS Software 5.2. The findings reveal clear diurnal variations with the lowest TEC was before dawn and a pronounced post-noon peak typically occurring around 08:00 UT. Equatorial TEC shows strong seasonal patterns, with peak values nearly twice as high during solar maximum periods compared to minima. There are two times each year when the TEC reaches its highest values, and these usually happen around March and September, which are the months of the equinoxes. A notable winter anomaly, where TEC in December(winter) is higher compared to TEC in June (summer), was also observed. Seasonal asymmetries including a reversal of equinoctial asymmetry in 2011, suggest additional geomagnetic influences. Correlation analyses demonstrate strong relationships between TEC and solar indices, particularly the PI index, which exhibits the highest correlation over the 12-year study period. Variations in correlation strength across solar cycle phases highlight the dynamic interplay between solar activity in affecting the equatorial ionosphere. By evaluating 12 years of data, this study provides valuable information and solid foundation for the ionospheric modelling and space weather forecasting.

Keywords: Total electron content; Equatorial ionosphere; Geomagnetic activity; Solar activity

1. INTRODUCTION

The ionosphere exhibits complex variations that are influenced by many factors including solar and geomagnetic activity. The ionosphere over the equatorial region is complex because it lies near the geomagnetic equator, where the magnetic field is almost horizontal, which makes studying it more challenging. Understanding the characteristic of ionosphere is crucial for both scientific research and practical applications, particularly through the analysis of ionospheric parameters such as Total Electron Content (TEC). TEC, defined as the total number of free electrons along the signal path between satellites and ground-based receivers, provides valuable information about regional ionization (Jayachandran et al., 2004, Pandit et al. 2021). A comprehensive study of climatology of TEC enables researchers to identify distribution patterns and better understand on how solar phenomena influence the ionosphere and its daily and annual variations.

Accurate TEC measurements play a pivotal role in satellite-based applications because the dispersive nature of the ionosphere leads to signal delays and phase advance, thus degrading positioning and communication system accuracy. Precise TEC estimation is therefore critical both for mitigating ionospheric errors in navigation systems and for investigating the ionospheric irregularities and disturbances such as scintillation, equatorial plasma bubble and Travelling Ionospheric Disturbance (TID) (Elmunim & Abdullah 2021, Falayi et al. 2024). These irregularities, along with the prominent

Equatorial Ionization Anomaly (EIA), pose unique challenges for stable ionospheric modeling and prediction, making the equatorial ionosphere compelling for scientific investigation.

Previous studies have consistently demonstrated that ionospheric Total Electron Content (TEC) exhibits strong seasonal variability that is closely modulated by solar activity. TEC typically follows a semiannual cycle, with higher values during the equinoxes, particularly the March equinox, compared to the September equinox, and minimum values during the solstices (Jayachandran et al., 2004; Liu et al., 2009). This semiannual variation is especially pronounced at low latitudes and is strongly influenced by the solar cycle, primarily through the equatorial fountain effect and changes in neutral atmospheric density (Liu et al., 2009). Region-specific studies further indicate that the ionospheric response to solar activity varies seasonally, with equinox periods exhibiting a more rapid and pronounced response to solar flux variations than solstices (Dashora & Suresh, 2015; Pandit et al., 2021). In addition, the absence of a winter anomaly at the dip equator during low solar activity conditions highlights the importance of regional and latitudinal factors in modulating TEC behavior (Dashora & Suresh, 2015).

In Malaysia, study on ionosphere using TEC commenced in the 1990s (Zain et al., 2008). Malaysia is in the equatorial region within 1°to 9°N, 97°to 120°E (geographical coordinate), close to the geomagnetic equator and at the trough of Equatorial Ionospheric Anomaly (EIA). Prior research identified daily TEC peaks in the afternoon and minimum in the early morning local time, with significant seasonal differences which is highest during equinoxes and lowest during soltices (Bahari & Abdullah, 2015; Leong et al., 2015; Musa et al., 2012). Another interesting phenomenon that was found is winter anomaly, where the TEC is higher in winter months which represent by December to January compared to June to July's summer. Other than that, Musa et al. (2012) reported that semiannual variation was more dominant compared to annual variation (Musa et al., 2012), while Bahari & Abdullah (2015) described in their study that during periods of low solar activity, a stronger correlation of daily TEC with solar flux was found compared to sunspot number and the geomagnetic index, whereas this correlation was weaker during high solar activity. These studies on the variations of TEC over Malaysia had investigated TEC during the rising phase (1998), maximum year for solar cycle 23 (2000), the decreasing phase (2003-2008), the minimum phase (2009-2010) and in 2011of solar cycle 23 (Bahari et al 2015). Moreover, these studies also utilised the data duration of one year up to nine years'; however, some researchers covered only one station (Bahari et al. 2015), other than Musa et al. (2012) who used the data from 78 GPS stations over Malaysia. However, past studies have generally been limited by fragmented data coverage, durations or reliance on single-station datasets, thus leaving considerable gaps in comprehensive understanding the ionospheric variability across equatorial especially Malaysia region.

To address these gaps, this study presents analysis of TEC variations in the equatorial region of Malaysia, spanning from the descending phase of solar cycle 23 which is year 2003 to 2005 to the peak phase of solar cycle 24 (2013–2014). This study examines diurnal variations, compares TEC during the equinoxes, and assesses variations during the solstices, thereby enhancing our understanding of the equatorial ionosphere's response to solar activity. On top of that, the relationship between TEC and four solar indices across different solar activity phases was also investigated.

2. MEASUREMENTS AND DATA COLLECTION

2.1 GPS-TEC Data

Bernese GNSS Software (BGS) version 5.2 was used to calculate the vertical TEC (VTEC) in this paper. BGS employed a geometry-free linear combination of pseudocode and phase. This combination removes errors related to the satellite and receiver clock biases, satellite orbit and station coordinate. The basic geometry-free combination is given by equation 1 and 2 below :

$$L_4 = L_1 - L_2 = \ -a\left(\frac{1}{f_1^2} - \frac{1}{f_2^2}\right) F_1(z) E(\beta, s) + B_4 \quad (1)$$

$$P_4 = P_1 - P_2 + a\left(\frac{1}{f_1^2} - \frac{1}{f_2^2}\right) F_1(z) B(\beta, s) + b_4 \quad (2)$$

where L_1 , L_2 represent carrier-phase and P_1, P_2 is pseudocode observations on the GPS frequencies f_1 = 1575.42 MHz and f_2 = 1227.60 MHz. Based on the equation, a : constant, 4.03 x 10^{17} $ms^{-2}TEC^{-1}$ while $F_1(z)$ represent the mapping function evaluated at the zenith distance, z'. $E(\beta,s)$ is the vertical TEC (VTEC), β is geographic latitude in this case, s is the longitude and $B_4 = \lambda_1 B_1 - \lambda_2 B_2$ is a constant bias of phase ambiguities, $b_4 = c(\Delta b^s + \Delta b_r)$, where Δb^s is satellite differential code bias and Δb_r is differential code bias for receiver. Single Layer Model (SLM) and spherical harmonic expansion approach was used in estimating the receiver biases dan VTEC. In this study, a thin-shell model with altitude of 450 km was used to convert the slant to the TEC. A comprehensive description of the SLM methodology and the derivation of vertical TEC is provided in Dach et al. (2018). This methodology has been widely applied in ionospheric studies over the Malaysian and equatorial regions (Zain et al. 2005, Ya;acob et al. 2008, Bahari et al. 2015, Mostafa et al. 2023).

This research utilizes GPS observational data in RINEX format from 2003 to 2014 were acquired from GPS receivers under the Department of Mapping and Surveying Malaysia (JUPEM) and additional stations under International GNSS Service (IGS) over South East Asia. Using data from these combined networks, TEC was estimated and mapped using BGS 5.2. It should be note that from 2003 to 2008, TEC maps covered latitudes ranging from 0° to 7°N and longitudes from 95° to 120°E, with a 1° increments for both latitude and longitude and 2-hour intervals, constrained by data availability at that time. Between 2009 and 2014, TEC mapping extended to cover latitudes from 0° to 9°N, maintaining the same longitudinal range (95° to 120°E), but with an improved temporal resolution of 1-hour intervals. For consistency in subsequent analysis, all TEC data were standardized to latitudes from 0° to 7°N and longitudes from 95° to 120°E with 2-hour intervals. The complete list of stations utilized in this study is shown in Figure 1. Analysis of TEC behavior over Malaysia was conducted by calculating the mean TEC, averaged across the latitudinal range from 0° to 7°N, following the method proposed by Liu et al. (2009). This method effectively captures general TEC behavior across the selected latitude range. Seasonal variation was analyzed by categorizing the data into three seasons: equinoctial seasons (March and September), winter (December), and summer (June). This categorization enables clear evaluation and comparison of seasonal influences on TEC variations in relation to solar activity.

The mean TEC for each year was computed using hourly averaged TEC values over Malaysia. For each month (e.g., March), TEC values were first averaged spatially over the Malaysian region at fixed local-time intervals. The diurnal variation was then represented using 12 local-time bins at 2-hour intervals (00, 02, …, 22 LT). For each local-time bin, TEC values were averaged over all available days within the selected month, resulting in 12 mean TEC values per year for that month. These 12 points therefore represent the monthly mean diurnal TEC variation at a 2-hour temporal resolution. The same averaging procedure was applied to all years of analysis and was also used in the subsequent analysis of TEC over Malaysia.

Figure 1 : GNSS receivers stations used in this analysis**.**

2.2 Solar Indices

In this study, four key parameters were selected to characterize solar activity: sunspot number, solar radio flux (F10.7), the solar activity factor (P index), and solar extreme ultraviolet (EUV) radiation. The sunspot number data were downloaded from the Royal Observatory of Belgium's website (https://sidc.be/). Solar radio flux measurements at a wavelength of 10.7 cm (F10.7) were sourced from NASA's OMNIWeb portal (https://omniweb.gsfc.nasa.gov). The P index was derived from the F10.7 data using the formula: P = (F10.7 + F10.7A) / 2, where F10.7A represents the 81-day centered average of F10.7 values. This method helps reduce short-term variability and enhances the correlation with ionospheric phenomena (Dashora et al., 2015; Chen et al., 2012). Both F10.7 and the P index were used to assess which solar activity parameter exhibits a stronger correlation with the mean TEC.. To represent the solar EUV component, data from the Solar EUV Monitor (SEM) onboard the Solar and Heliospheric Observatory (SOHO) were utilized (Judge et al., 1998). In this paper, SEM EUV data used correspond to central-order EUV flux within the 0.1–50 nm wavelength range, recorded at 1 AU with daily resolution and can be download from the LASP Interactive Solar Irradiance Datacenter (LISIRD) via this link : https://lasp.colorado.edu/lisird/.

3. RESULTS AND DISCUSSION

In the following sections, details on diurnal, seasonal variations and TEC dependence to solar activity are presented. The main features of TEC such as seasonal anomalies and equinoctial asymmetries in the equatorial region are discussed. According to Hathaway and Suess (2008), solar cycle 23 start in 1996 with the minimum between Cycle 22 and Cycle 23 occurring in September 1996. Figure 2 shows an overview of solar activity during solar cycle 23 (1996 – 2008) and the ascending phase of solar cycle 24 (2008 to 2014).

Panel (a) of Figure 2 shows daily (gray line) and monthly averaged (blue line) sunspot numbers, which reflecting the variability and general trend of solar activity. Panel (b) depicts the daily solar flux at 10.7 cm wavelength (F10.7, gray line), a solar activity indicator, along with the P index (blue line). The period from 2003 to 2014, as highlighted in light green was selected for analysis due to its coverage of declining phase, solar minimum and early ascending phase, which are particularly relevant for studying the ionospheric respond to the solar influences.

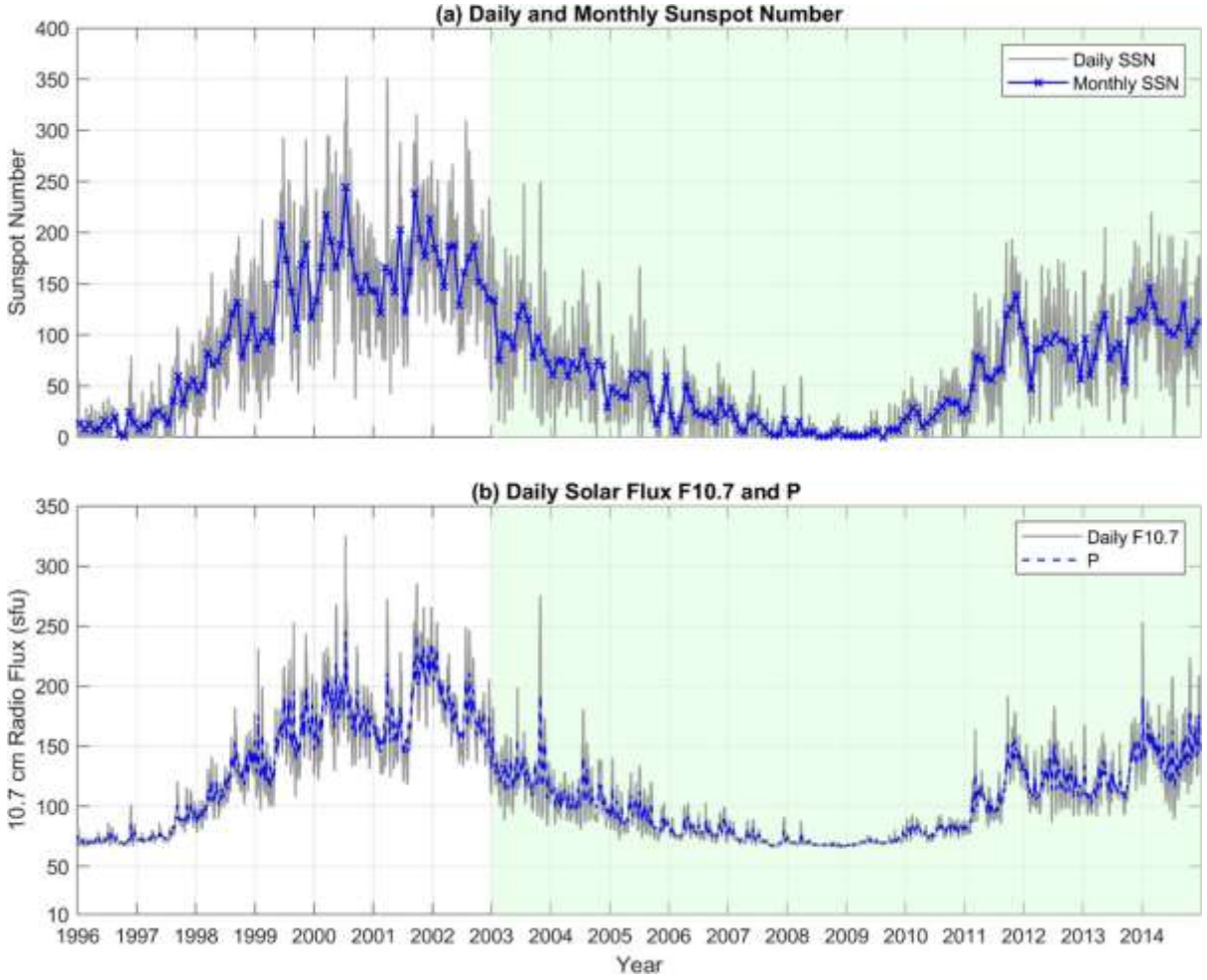

Figure 2 : Solar indices during solar cycle 23 from 1996 to 2008 and increasing phase of solar cycle 24 (2008 to 2014). Panel (a) shows the daily sunspot number (gray line) and monthly sunspot number (blue line). Panel (b) shows daily F10.7 flux (gray line) and P index (blue line). Each year tick marks January 1st. The light green shaded region (2003–2014) indicates the period of year that were analyzed in this study, corresponding to the declining phase, minimum and increasing phase of solar activity.

3.1 General Variation of Diurnal TEC

Figure 3 presents the mean daily TEC for January to December from 2003 to 2014. The plot displays a two-dimensional map of month versus Universal Time (UT), with TEC values averaged for every two hours. This method aims to capture the diurnal variations of TEC under varying solar conditions. The color bar indicates TEC values ranging from 0 to 100 TECU. A typical diurnal patter of TEC over equatorial region is evident with minimum during early morning and maximum around post-noon. A high TEC was observed between 0400 UT to 1000 UT, with peak values occurring around 0800 UT. Furthermore, Figure 3 demonstrates that TEC during equinoctial months (March and September) were generally higher TEC than during solstice months, reflecting the semiannual variation. Moreover, the March equinox consistently exhibit higher TEC than the September equinox (except in 2008 and 2009), highlighting the phenomenon of equinoctial asymmetry. In 2008 and 2009, the TEC differences between equinoxes were minimal. Daily variation of TEC in the equatorial region is influenced by solar flux, geomagnetic activity, equatorial electrojet dynamics and thermospheric conditions (Patari et al. 2021).

Diurnal TEC variations for 12 years' analysis also show seasonal dependencies in peak timing and amplitude. During equinox periods (March–April and September–October), the peak TEC generally occurs earlier, typically between 0600 UT to 0800 UT, reflecting enhanced solar ionization and stronger

equatorial electrodynamics. In contrast, during solstice seasons, particularly the June solstice, the TEC maximum tends to occur later in the afternoon, around 0800 to 0900 UT, and is generally weaker in magnitude. This shift in peak timing is more pronounced during years of high solar activity (2003–2004 and 2013–2014), while during low solar activity years (2008–2009), the diurnal peak is less distinct and shows reduced seasonal contrast. During periods of decreasing phase of solar activity or low solar activity, such variations are largely driven by extreme ultraviolet (EUV) radiation and its coupling with neutral atmospheric dynamics. Interactions between zonal and meridional winds and ionospheric plasma complicate the modeling of both short-term and long-term variations (Dashora et al., 2015).

In Figure 3, TEC values were notably higher during the March to April and September to October periods, with a consistently stronger peak observed in March to April. The lowest TEC values were primarily recorded during the solstice months, namely June and July as well as December, supporting the well-known semiannual variation pattern. To better examine these seasonal trends, the TEC distribution was analyzed by comparing the equinoxes (March versus September) and the solstices (June versus December). The observed asymmetries, particularly between the equinox periods, will be further discussed in the following section.

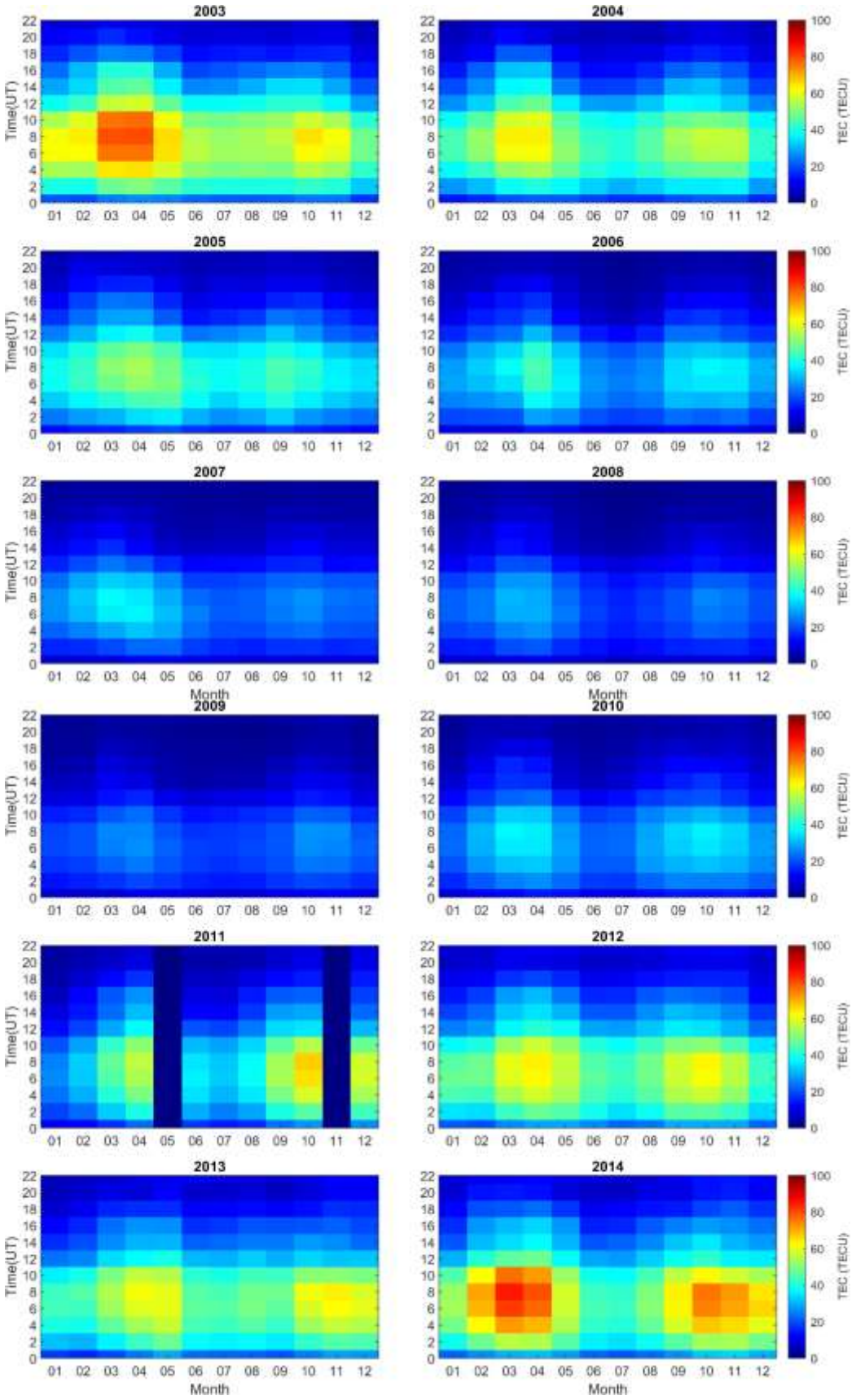

Figure 3: A two-dimensional variation of hourly mean TEC over equatorial region from 2003 to 2014.

3.2 Seasonal Variations of TEC

Figure 3 shows that the TEC at the equatorial region shows a clear seasonal variation. During the periods of high solar activity, for example the year 2003 and 2014, the maximum value of TEC was nearly double that observed during low solar activity which represents by the year of 2008 and 2009. The maximum TEC in 2003 was during high solar activity was about 80 TEC and 2014 is 85 TECU while during solar minimum (2008), the maximum of TEC is around 35 TECU. There were two signatures of high TEC around March and September each year, which were observed from Figure 3, corresponding to the equinoxes. In contrast, the lowest TEC values are generally recorded during June and July, the summer solstices months.

According to Jonah et al. (2015), during solstices, the overhead Sun shifts to higher latitudes, reducing photoionization at the equator. To assess seasonal differences, this paper focuses on equinoxes and solstices season. The data were categorized into four parts. Figure 4(a) presents the mean TEC for March and September, while Figure 4 (b) illustrates the difference between these two months from 2003 to 2014. TEC in March exhibited higher TEC values than September during the decreasing phase of solar cycle (2003 to 2005), the solar minimum (2007 – 2009), and the solar maximum (2013-2014). An exception was 2011, where TEC in September was higher compared to March, indicating a reversal of equinoctial asymmetry. This reversal is consistent with findings by Dashora & Suresh (2015).

The reversal of the equinoctial asymmetry where TEC in the September equinoxes was higher compared to the March equinoxes that occurred during 2011. Seasonal TEC variations over the equatorial region are also known to be strongly influenced by the strength of the equatorial electrojet (EEJ), which modulates ionospheric plasma transport and distribution (Bagiya et al., 2009). In addition to electrodynamic processes, geomagnetic disturbance may also have contributed to the observed reversal in 2011. Geomagnetic disturbance is known to significantly perturb equatorial ionospheric conditions through storm-time electric fields and changes in thermospheric composition, which can lead to enhanced or redistributed TEC.

To examine whether geomagnetic activity differed between the two equinox months in 2011, the Dst index (World Data Center for Geomagnetism, Kyoto) was analysed, and hours with Dst < −50 nT were classified as geomagnetically disturbed. In this study, the Dst index was collected from World Data Center for Geomagnetism (WDC - https://wdc.kugi.kyoto-u.ac.jp/index.html). Figure 5 compares the hourly Dst variation for March and September 2011, where black markers represent March and the blue line represents September. The September equinox exhibits more frequent and stronger negative Dst excursions than in March, including a pronounced disturbance episode late in the month. This suggests that the elevated geomagnetic disturbance level during September 2011 could have contributed to the enhanced TEC during that equinox and may be one factor associated with the observed reversal of equinoctial asymmetry. However, a detailed quantification of storm-time effects on TEC is beyond the scope of this paper and is not examined further here.

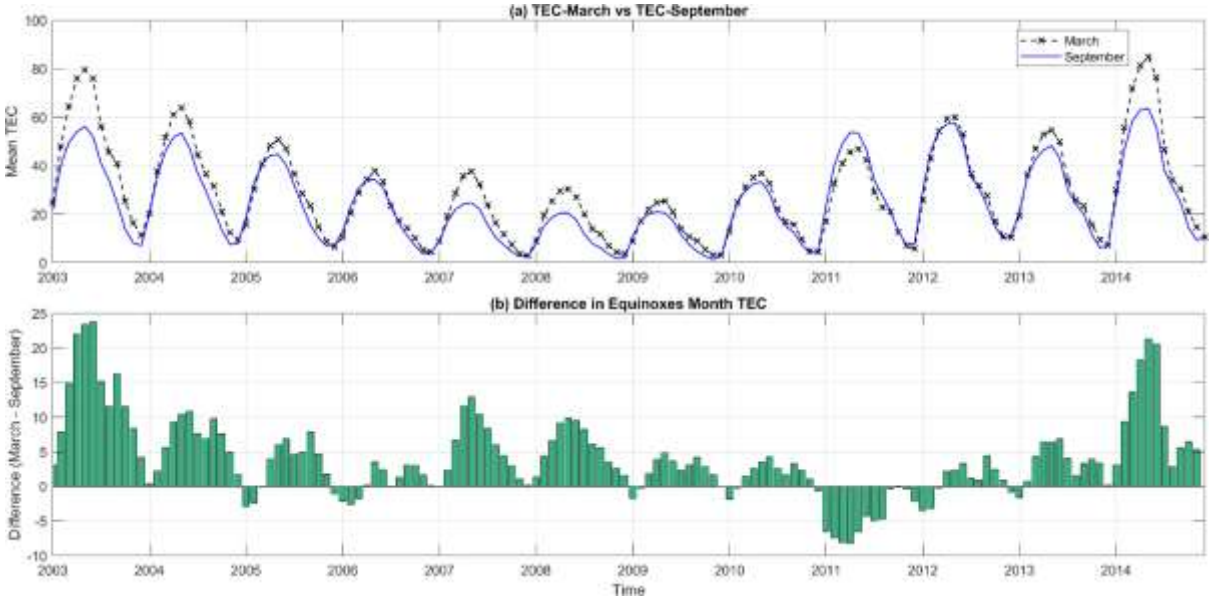

Figure 4 : (a) Mean TEC for March and September and (b) the difference of TEC in March compared to September from 2003 to 2014.

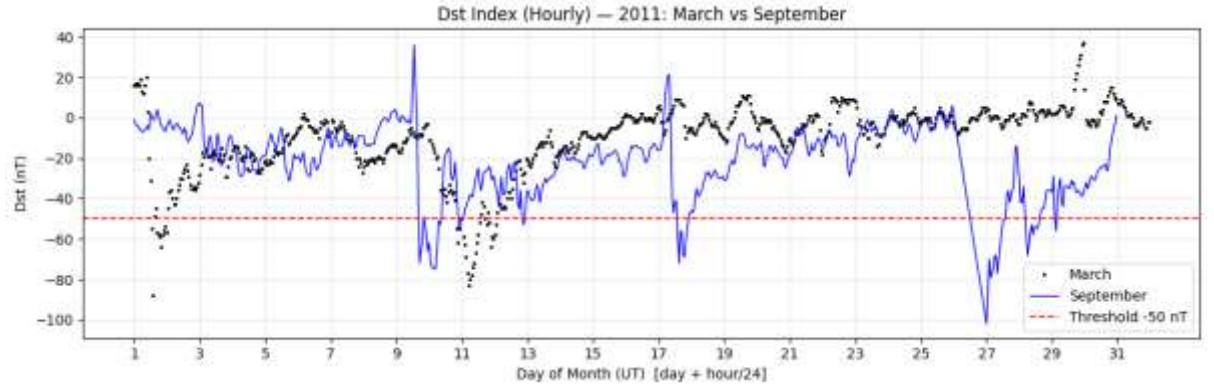

Figure 5: Comparison of hourly geomagnetic conditions in March and September 2011 based on the Dst index. Black markers represent March, while the blue solid line represents September. The red dashed line denotes the disturbance threshold at −50 nT.

High TEC was recorded during equinoxes compared to summer and winter based on Figure 3 and Figure 4. It can also be observed that mean TEC value during winter solstice (December) was higher compared to summer solstice (June) starting from 2006. This observation is considered a winter anomaly. Winter anomaly occurs if maximum TEC in winter is higher than summer (Huo et al., 2009). Mean TEC during equinoxes is higher at more than 5 to 20 TECU (ranging depends on solar activity) throughout the years while a difference of ~ 2 TECU to more than 20 TECU was observed between summer and winter solstice.

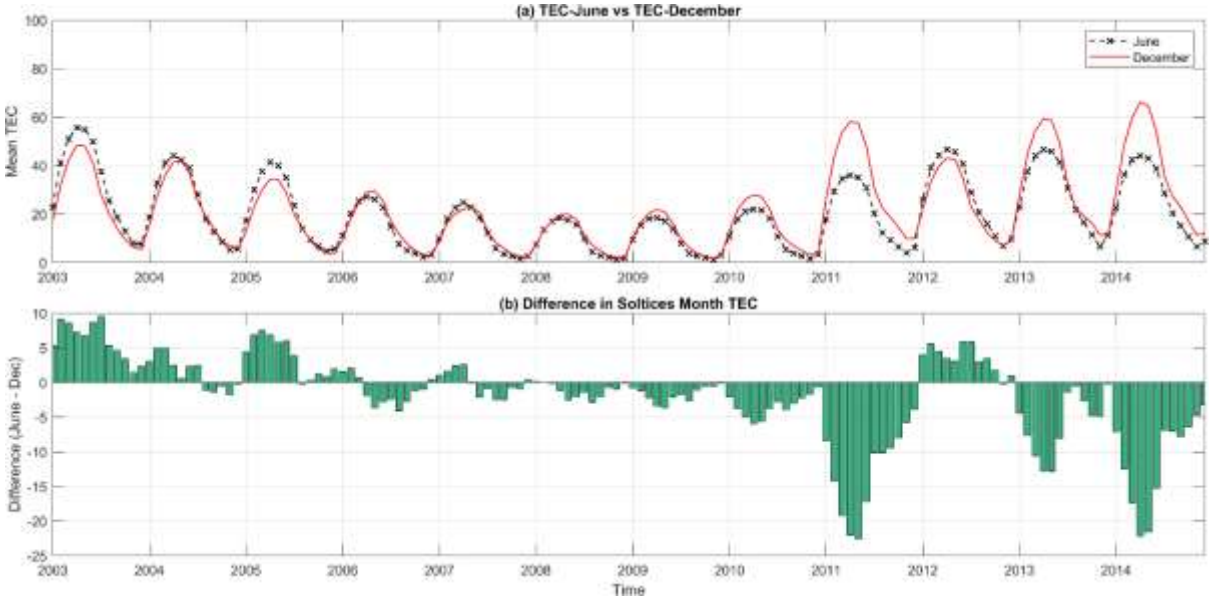

Figure 6 : (a) Mean TEC for July and December and (b) the difference of TEC in July compared to December from 2003 to 2014.

Figure 6(a) compares the TEC for July and December and Figure 6(b) illustrates the TEC difference between the months. A winter anomaly, defined as a pronounced and persistent enhancement of December TEC relative to June. The winter anomaly was evident starting 2008 to 2011 and 2013 - 2014, but absent in 2003 to 2005 and 2012. In 2011 and 2014, December TEC consistently exceeds June TEC, indicating a well-developed winter anomaly over the equatorial Malaysian region. In contrast, during 2003–2005 and 2012, June TEC remains comparable to or higher than December TEC, suggesting the absence of a winter anomaly. Although differences between June and December are visible in 2007, the magnitude of the enhancement is relatively small and not persistent across all local times. These years therefore represent weak or transitional behavior, rather than a distinct winter anomaly. Dashora and Suresh (2015) reported the disappearance of the winter anomaly during 2003–2008, while Zhang et al. (2014) observed winter anomalies at low latitudes during 2005–2009. Such discrepancies highlight the strong influence of regional and seasonal thermospheric conditions, including variations in neutral composition (O/N_2 ratio), meridional winds, and electrodynamic processes, on the development of the winter anomaly.

These results indicate that, at equatorial latitudes, the occurrence of the winter anomaly is not solely controlled by solar activity. Instead, it is modulated by a combination of solar forcing and regional thermospheric–ionospheric coupling. When solar activity falls below a certain threshold, the winter anomaly may weaken or disappear, as suggested by Burns et al. (2014). To further investigate the role of solar activity into the variation of TEC over Malaysia, the relationship between solar activity parameters and mean TEC is examined in the following section.

3.4 Variations of TEC with Solar Indices

To examine the dependence of TEC on solar activity, daily mean TEC was compared with several solar activity indices, including sunspot number, F10.7 index, P index, and EUV radiation. As shown in Figure 7, the daily variations in TEC closely follow the trends observed in these solar indices, demonstrating a consistent agreement across the dataset from 2003 to 2014. The modulation of TEC in response to solar rotation, reflected in both sunspot numbers and the F10.7 index, provides strong evidence for the influence of solar irradiance on the ionosphere.

A correlation analysis was done to quantify the consistency between TEC and solar activity by calculating correlation coefficients. The Pearson correlation coefficient (r) was employed to assess the

strength of association, with values of r greater than 0.7 interpreted as indicating a strong correlation. A linear relationship was evaluated through polynomial fitting. Figure 8 illustrates the dependency of daily TEC on various solar activity indices, including sunspot number, solar radio flux (F10.7), P), and the SOHO/SEM EUV index (hereafter referred to as EUV). The analysis reveals a strong linear correlation between daily mean TEC and all indices, with r values exceeding 0.7 for all parameters except the EUV index, which yielded a slightly lower value of 0.67. Despite being below the 0.7 threshold, this still suggests a statistically meaningful correlation.

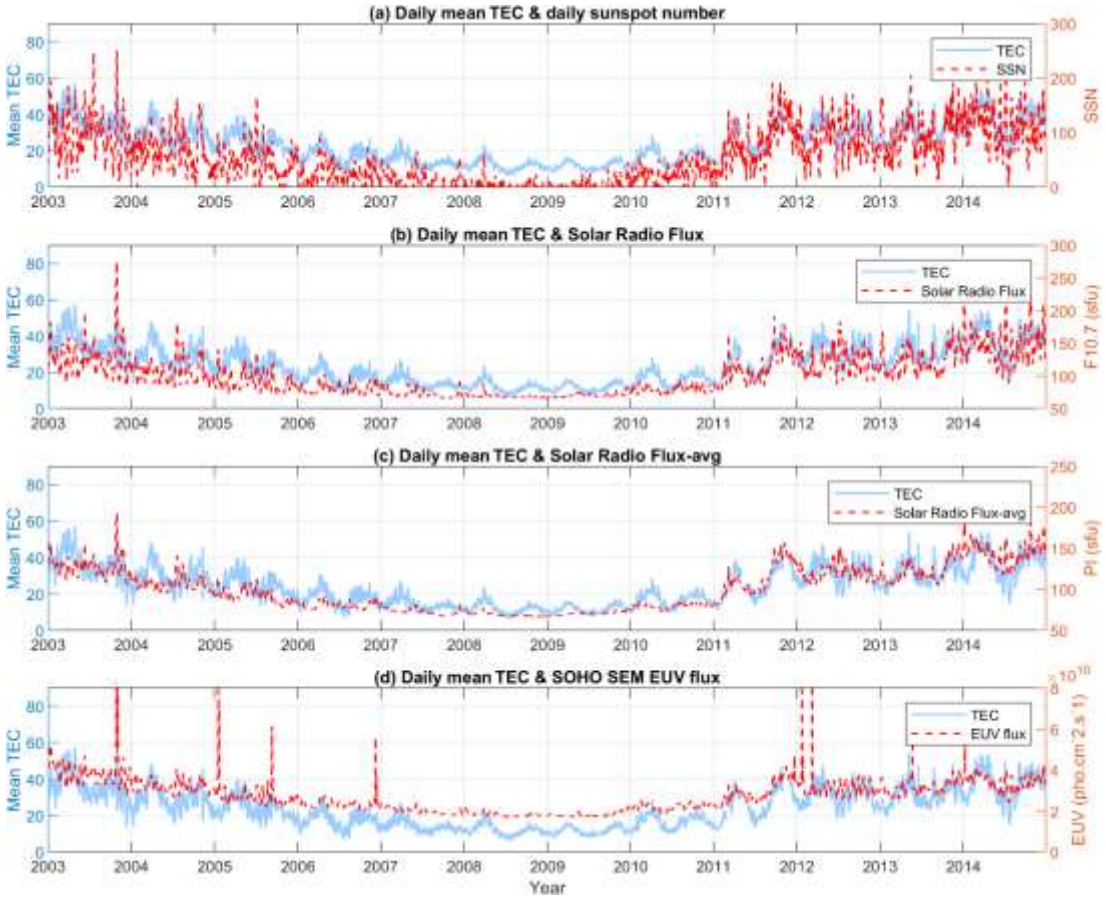

Figure 7 : Daily mean TEC with the four solar indices (a) daily sunspot number, (b) solar radio flux, F10.7, (c) PI and (d) EUV for 2003 to 2014.

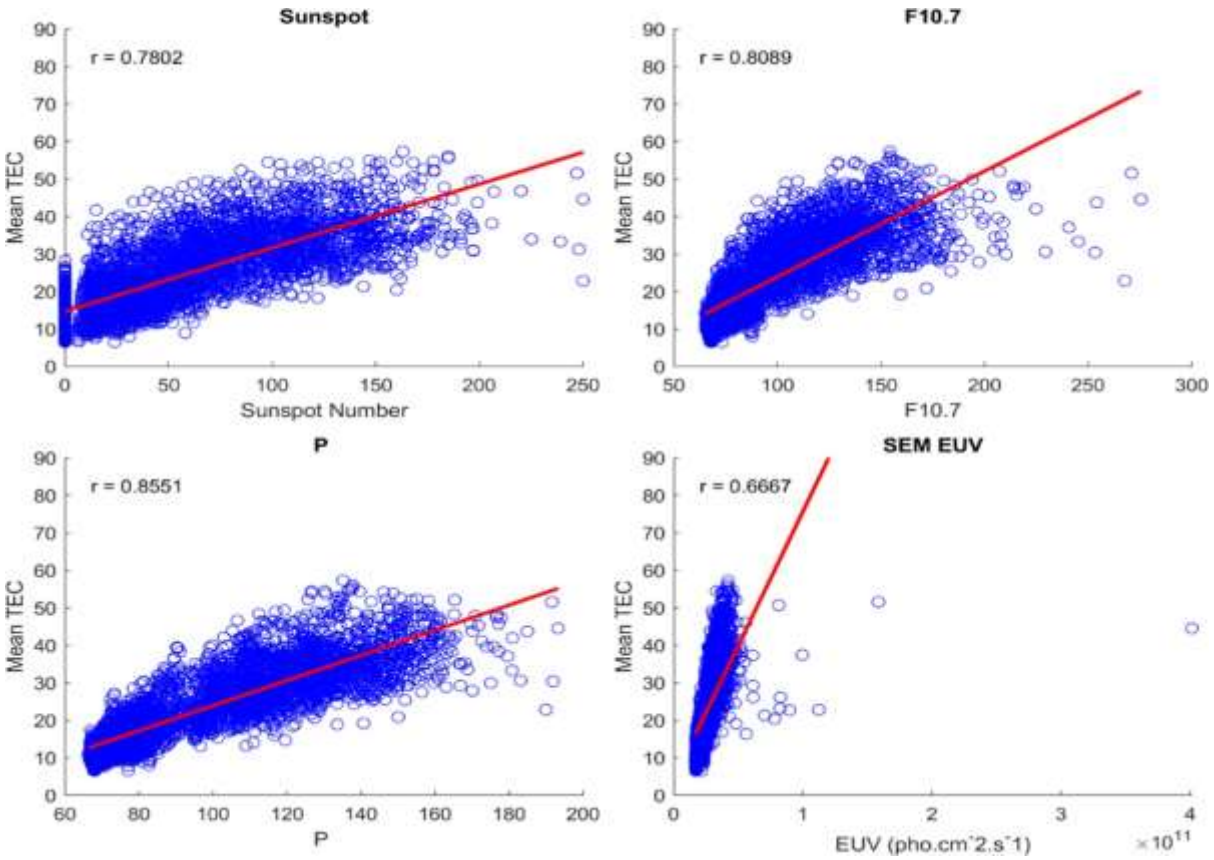

Figure 8 : The dependence of daily mean TEC with the sunspot number, F10.7, P and SOHO SEM EUV 0.1 – 50 nm).

The dependence of daily mean with those indices were also calculated for different phase of solar activity to further study the correlation of daily mean TEC with the solar activity indices. The data has been divided into five categories which are (i) all data coverage, (ii) declining phase of solar cycle (2003 to 2005), (iii) solar minimum (2007 to 2009), (iv) rising phase (2010 to 2012) and solar maximum phase (2013 to 2014). The level of correlation is based on the Feng et al (2023) where the value of correlation, r is -1 to 1. The correlation between parameters is considered extremely high if the r is between 0.7 to 1 and lower if the value of r is closer to 0. Based on this configuration, results on the correlation analysis are presented in Figure 9 where the color bar ranges from 0 to 1, representing the strength of the correlation. Across the full period of analysis, the correlation between TEC and all indices is generally strong, with the PI showing the highest correlation (r = 0.84), followed by F10.7 (r = 0.77), sunspot number (r = 0.74), and the EUV index is 0.61. These results reflect a consistent relationship between TEC and solar activity over the long term. Generally, from Figure 9, it can be seen that the correlation is strong during ascending phase of solar activity which represents by the year of 2010 to 2012 and weakest during the minimum phase of solar activity.

All correlation values are less than 0.7 in 2003 to 2005, during the descending phase of solar cycle 23, indicating a weakening in TEC's dependence on solar parameters during periods of decreasing solar activity. This trend is especially evident in the EUV index, with a correlation of just r = 0.37. In the solar minimum period which cover year of 2007 to 2009, correlations are significantly low across all indices, with the sunspot number (r = 0.16), F10.7 (r = 0.24), and PI (r = 0.30) showing weak relationships with TEC. Interestingly, the EUV index shows a slightly higher correlation where r = 0.44, suggesting that even during minima, EUV emissions may continue to play a role in ionospheric variability.

For the year 2010 to 2012, which is during the ascending phase of solar cycle 24, correlations strengthen markedly, especially for PI, where the r = 0.82, F10.7 with r = 0.78 and sunspot number, r = 0.77, reinforcing the idea that TEC is strongly modulated by increasing solar activity. The EUV index

also shows an improved correlation, r = 0.67, near the strong correlation threshold. In the solar maximum period (2013–2014), moderate correlations are observed, with values ranging from r = 0.46 (sunspot number) to r = 0.64 (PI). The EUV index shows a slightly improved correlation (r = 0.63) compared to earlier phases, possibly reflecting the intensified and more variable ionizing radiation during peak solar activity.

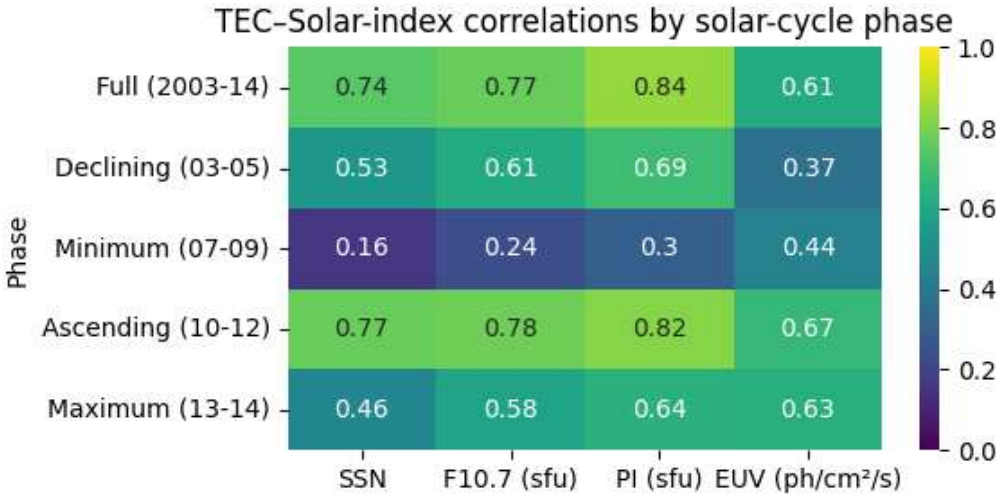

Figure 9 : Correlation coefficients of daily mean TEC sunspot number, F10.7, PI and EUV 0.1 – 50 nm

4. CONCLUSIONS

This study examined mean Total Electron Content (TEC) over the equatorial region from 2003 to 2014. The results show that mean TEC closely follows solar variability: it tracks the solar cycle variability and the semiannual oscillation. A consistent diurnal pattern emerged throughout the data set, with a minimum just before dawn and a peak after local noon. Equinox months always exhibited the highest TEC, and equinoctial asymmetry persisted across the entire 12-year record except for 2011. A winter anomaly appeared only during the solar-minimum, rising, and maximum phases—except in 2012. These findings is interesting to be further analyzed. Altogether, these findings confirm that mean TEC is a valuable ionospheric proxy for monitoring solar-driven changes as a new solar cycle begins. Future work should incorporate additional solar-activity indices and other geophysical drivers, using advanced statistical or alternative analytical methods, to deepen our understanding of equatorial ionospheric behavior and improve predictive models

5. REFERENCES

Akir, R.M., Chellappan, K & Abdullah, M. (2017). Total Electron Content forecasting using Artificial Neural Network. *Pertanika Journal of Science and Technology*, 25 (S). 19-28.

Aderaw, B. and Nigussie, M. (2025). Statistical study on the effect of meridional neutral wind on the occurrence of post-sunset equatorial ionospheric irregularities. *Space Weather*, 23(1). E2024W003872.

Afraimovich, E. L., Astafyeva, E. I., Oinats, A. V. et al. (2008). Global electron content: A new conception to track solar activity. *Ann.Geophysc*., 26, 335 - 344.

Bagiya, M., Joshi, H. P., Iyer, K. N. et al. (2009). Tec variations during low solar activity period (2005–2007) near the equatorial ionospheric anomaly crest region in india. *Ann. Geophys*., 27, 1047–1057.

Bahari, S., & Abdullah, A. M., M.and Hasbi (2015). A review of ionospheric studies in Malaysia using GPS. In Proceeding of the 2015 International Conference on Space Science and Communication (IconSpace) (pp. 95–100).

Burns, A. G., Wang, W., Qian, L. et al. (2014). On the solar cycle variation of the winter anomaly. J. Geophys. Res. Space Physics, 119, 4938–4949.

Chen, Y., Liu, L. and W, Wan. 2012. The discrepancy in solar EUV-proxy correlations on solar cycle and solarrotation timescales and its manifestation in the ionosphere, *J. Geophys. Res*., 117, A03313.

Dach, R., Lutz, S., Walser, P. et al. (2015). In Bernese GNSS Software 5.2 (p. 514 - 852).

Dashora, N., & Suresh, S. (2015). Characteristic of low-latitude tec during solar cycles 23 and 24 using global ionospheric maps (gims) over indian sector.*J. Geophys. Res. Space Physics*, 120, 5176–5193.
Elmunim, N.A. & Abdullah, M (2021). Ionospheric delay investigation and forecasting, Springer, SpringerBriefs in Applied Sciences and Technology, Singapore
Falayi, E.O., Amaechi, P.O (2024). Analysis of total electron content over the African low-latitude region during the maximum phase of solar cycle 24 (2012-2014). Journal of Atmopsheric and Solar-Terrestrial Physics, 258, 106235.
Feng, J., Zhang, Y., Li, W., Han, B., Zhao, Z. Zhang, T. & Huang, R. (2023). Analysis of ionospheric TEC response to solar and geomagnetic activities at different solar activity stages. Advances in Space Research, 71, 2225-2239.
Hathaway, D. H., and S. T. Suess (2008), Solar cycle 23, in The Heliosphere Through the Solar Activity Cycle, edited by A. Balogh et al., pp. 21–39, Praxis, Chichester, U. K.
Hocke, K. (2008). Oscillations of global mean tec. *J. Geophys. Res. Space Physics*, 113, A04302.
Huo, X. L., Yuan, Y. B., Ou, J. K. et al. (2009). Monitoring the global-scale winter anomaly of total electron contents using gps data. *Earth Planet Space*, 61, 1019–1024.
Jayachandran, B., Krishnankutty, T. N., & Gulyaeva, T. L. (2004). Climatology of ionospheric slab thickness. *Ann. Geophys.*, 22, 25–33.
Jonah, O. 526 F., de Paula, E. R., Muella, M. T. A. H. et al. (2015). Tec variation during high and low solar activities over south american sector. *J. Atmos. Sol. Terr. Phys.*, 135, 22–35.
King, J. H., and N. E. Papitashvili (2005), Solar wind spatial scales in and comparisons of hourly Wind and ACE plasma and magnetic field data, *J. Geophys. Res*., 110, A02104,
Leong, S. K., Musa, T. A., Omar, K. et al. (2015). Assessment of ionosphere models at banting : Performance of iri-2007, iri-2012 and nequick 2 models during the ascending phase of solar cycle 24. *Adv. Space Res.*, 55, 1928–1940.
Liu, L., Le, H., Chen, Y. et al. (2011). Features of the middle- and loaw-latitude ionosphere during solar minimum as revealed from cosmic radio occultation measurements. *J. Geophys. Res. Space Physics*, 116, A09307.
Liu, L.,Wan, W., Ning, B. et al. (2009). Climatology of the mean total electroncontent derived from gps global ionospheric maps. *J. Geophys. Res. Space Physics*, 114, A06308.
Mostafa, S., Abdullah, M., Bahari, S.A. and Islam, M.T. 2023. Analysis of the regional ionospheric disturbance index during geomagnetic storm in 2012. *IEEE Access*, 11, 94742 – 94752.
Mukherjee, S., Sarkar, S., Purohit, P. et al. (2010). Seasonal variation of total electron content at crest of equatorial anomaly station during low solar activity conditions. *Adv. Space Res*., 46, 291–295.
Musa, T. A., Leong, S. K., & Abdullah, R., A.and Othman (2012). Iskandarnet iomos near real-time equatorial space weather monitoring and alert system in peninsular malaysia. *Space Weather*, 10, S11003.
Pandit, D., Ghimire, B., Amory-Mazaudier, C., Fleury, R., Chapagain, N.P. & Adhikari, B. (2021). Climatology of ionosphere over Nepal based on GPS total electron content data from 2008 to 2018. Annales Geophysicae, 39, 743 – 758.
Pesnell, W. (2016). Prediction of solar cycle 24 : How are we doing? *Space Weather*, 14, 10–21.
Qian, L., Burns, A. G., Solomon, S. C. et al. (2013). Annual/semiannual varia5tions of the ionosphere. *Geophys. Res. Lett.*, 40, 1928–1933.
Scharroo, R., & Smith, W. H. F. (2010). A global positioning system-based climatology for the total electron content in the ionosphere. *J. Geophys. Res*, 115, 10318.
Tsai, H. F., Liu, J. Y., Tsai, W. H. et al. (2001). Seasonal variations of the ionospheric total electron content in asian equatorial anomaly regions. *J. Geophys. Res,* 106, 30363–30369.
Vaishnav, R., Jacobi, C., Berdermann, J., Schmölter, E., Dühnen, H., & Codrescu, M. (2024). Ionospheric response to solar EUV radiation variations using GOLD observations and the CTIPe model. *Journal of Geophysical Research: Space Physics*, 129, e2022JA030887
Vaishnav, R., Jacobi, C. & Berdermann, J. (2019). Long-term trends in the ionospheric response to solar extreme-ultraviolet variations. Annales Geophysicae, 37, 1141-1159.
Woldermariam, S.W. & Gogie, T.K. (2024). Characterize the long-term ionospheric response to the changes in solar activity at low-latitude stations of the East African Sector. Advances in Space Research, 73, 1875 – 1892.
Ya'aacob, N., Abdullah, M., Ismail, M., Bahari. S.A and Ismail, M.K. (2008). Ionospheric mapping function for total electron content (TEC) using Global Positioning System (GPS) data in Malaysia, *2008 IEEE International RF and Microwave Conference*, Kuala Lumpur, Malaysia, 386 – 390.
Yu, T., Wan, W., Liu, L. et al. (2004). Global scale annual and semi-annual variations of daytime nmf2 in the high solar activity years. *J. Atmos. Sol. Terr. Phys.*, 66, 1691–1701.
Zain, A., Abdullah, S., Homan, M. et al. (2008). Observations of the f3-layer at equatorial region during 2005. *J. Atmos. Sol. Terr. Phys*., 70, 918–925.
Zain, A..F.M.., Ho, Y.H. and Harun, H. (2005). Mapping of the Malaysian regional total electron content (TEC) latitude and longitude profile. *Journal of The Institution of Engineers, Malaysia*, 66(3), 8-13.

Zhang, X., Shen, X., Liu, J. et al. (2014). The asymmetrical features in electron density during extreme solar minimum. *Adv. Space Res.*, 54, 2236–2248.
Zhao, B., Wan, W., Liu, L. et al. (2007). Features of annual and semiannual variations derived from the global ionospheric maps of total electron content. *Ann. Geophys.*, 25, 2513–2527.

Acknowledgments
The GPS data was collected from the Department of Survey and Mapping Malaysia (JUPEM). This work was supported by GUP-2020-075 University Grant (GUP) and ZF-2024-004 made available through Universiti Kebangsaan Malaysia.